ROYAL SOCIETY OPEN SCIENCE

royalsocietypublishing.org/journal/rsos

Research

Cite this article: Clark B, Elkin J, Marconi A, Turner GF, Smith AM, Joyce D, Miska EA, Juntti SA, Santos ME. 2022 *Oca2* targeting using CRISPR/Cas9 in the Malawi cichlid *Astatotilapia calliptera*. *R. Soc. Open Sci.* **9**: 220077. https://doi.org/10.1098/rsos.220077

Received: 20 January 2022
Accepted: 22 March 2022

Subject Category:
Organismal and evolutionary biology

Subject Areas:
genetics/evolution/developmental biology

Keywords:
cichlids, CRISPR/Cas9, adaptive radiation, functional genetics, evo-devo

Author for correspondence:
M. Emília Santos
e-mail: es754@cam.ac.uk

†These two authors contributed equally to this work.

Electronic supplementary material is available online at https://doi.org/10.6084/m9.figshare.c.5937119.

THE ROYAL SOCIETY PUBLISHING

Oca2 targeting using CRISPR/Cas9 in the Malawi cichlid *Astatotilapia calliptera*

Bethan Clark[1,†], Joel Elkin[1,†], Aleksandra Marconi[1], George F. Turner[3], Alan M. Smith[4], Domino Joyce[4], Eric A. Miska[2,5,6], Scott A. Juntti[7] and M. Emília Santos[1]

[1]Department of Zoology, and [2]Department of Genetics, University of Cambridge, UK
[3]School of Natural Sciences, Bangor University, Gwynedd LL57 2TH, UK
[4]Department of Biological and Marine Sciences, University of Hull, UK
[5]Gurdon Institute, University of Cambridge, Cambridge CB2 1QN, UK
[6]Wellcome Sanger Institute, Wellcome Trust Genome Campus, Cambridge, UK
[7]University of Maryland, USA

DJ, 0000-0002-4253-5623; MES, 0000-0003-3158-7935

Identifying genetic loci underlying trait variation provides insights into the mechanisms of diversification, but demonstrating causality and characterizing the role of genetic loci requires testing candidate gene function, often in non-model species. Here we establish CRISPR/Cas9 editing in *Astatotilapia calliptera*, a generalist cichlid of the remarkably diverse Lake Malawi radiation. By targeting the gene *oca2* required for melanin synthesis in other vertebrate species, we show efficient editing and germline transmission. Gene edits include indels in the coding region, probably a result of non-homologous end joining, and a large deletion in the 3′ untranslated region due to homology-directed repair. We find that *oca2* knock-out *A. calliptera* lack melanin, which may be useful for developmental imaging in embryos and studying colour pattern formation in adults. As *A. calliptera* resembles the presumed generalist ancestor of the Lake Malawi cichlid radiation, establishing genome editing in this species will facilitate investigating speciation, adaptation and trait diversification in this textbook radiation.

1. Introduction

Identifying the genetic and developmental mechanisms underlying novel and variable morphologies is key to understanding how diversity arises in nature. Instances of adaptive radiation, that is, the rapid formation of an abundance of diverse species from a common ancestor, are perfect systems to delve into the basis of diversification and adaptation to distinct ecological niches [1].

© 2022 The Authors. Published by the Royal Society under the terms of the Creative Commons Attribution License http://creativecommons.org/licenses/by/4.0/, which permits unrestricted use, provided the original author and source are credited.

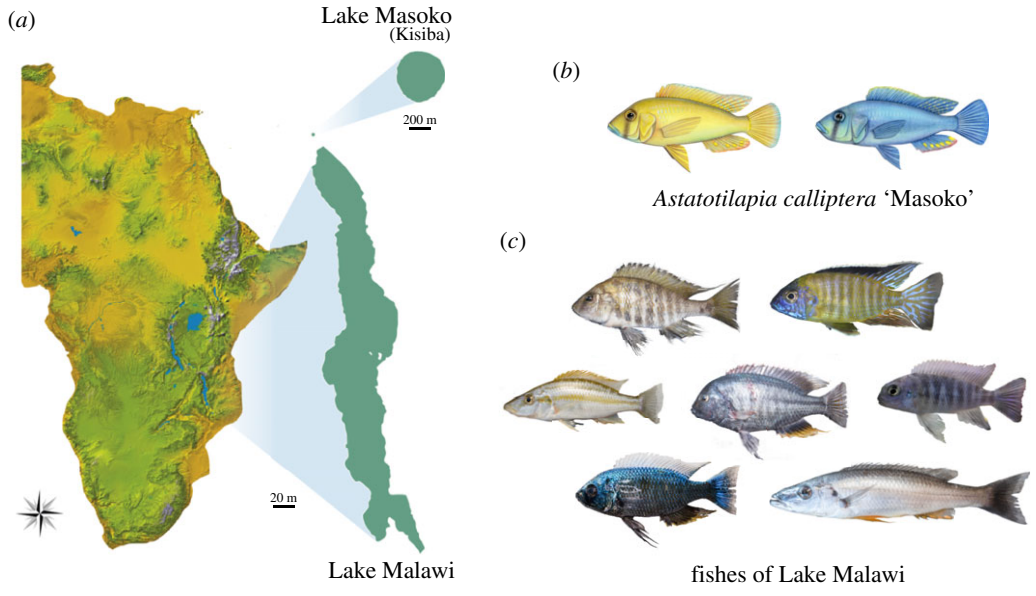

Figure 1. *Astatotilapia calliptera* and Malawi cichlids. (*a*) Geographical location of Lake Malawi and Lake Masoko/Kisiba. Map diagram courtesy of Gregóire Vernaz. (*b*) The two *A. calliptera* ecomorphs from Lake Masoko/Kisiba. Drawings by Julie Jonhson. (*c*) A snapshot of the diversity of forms present in Lake Malawi. Photographs courtesy of Hannes Svardal.

Cichlid fishes are a textbook example for such adaptive radiations. They are one of the most species-rich vertebrate families comprising over 2200 species which exhibit extraordinary morphological, physiological and behavioural variation [2–4]. The majority of species (approx. 2000) are found in the East African lakes, Tanganyika, Victoria and Malawi. Lake Malawi alone has over 800 species that emerged in the last 800 000 years [4,5]. They show extensive morphological variation in body shape, craniofacial skeleton, jaw apparatus, lateral line system, brain, vision and pigmentation phenotypes among other traits [6–13]. Despite their morphological diversity, the average sequence divergence between Malawi cichlid species pairs is only 0.1–0.25%, thus within this lake the evolution of divergent phenotypes seems to occur through comparatively minor genetic changes [5,14]. Their genetic similarity enables interspecific hybridization, which can be used for quantitative trait loci analysis to uncover genes underlying variation in species-specific traits. This is bolstered by their amenability to the laboratory and the wealth of genomic resources that have been made available in recent years, including many representative reference genomes [15]. While the aforementioned tools facilitate the discovery of loci associated with trait diversification, proof of causality can only be achieved by testing candidate gene function through genome editing.

Here, we report the application of CRISPR/Cas9 to generate coding and non-coding sequence mutants in the cichlid *Astatotilapia calliptera*, a maternal mouthbrooder cichlid fish that is part of the Malawi haplochromine radiation. *A. calliptera* occupies a rich diversity of habitats, including Lake Malawi, as well as peripheral rivers and lakes [16]. Phylogenetic analysis shows that all Malawi cichlid species can be grouped into seven eco-morphological groups, resulting from three separate cichlid radiations that stemmed from a generalist *Astatotilapia*-type ancestral lineage [5]. As such, *A. calliptera* is a useful model in which to develop functional tools to explore Malawi cichlid speciation and adaptation (figure 1). We specifically focused on one *A. calliptera* population from a small crater lake situated north of Lake Malawi (figure 1*a*) referred to in the literature as Lake Masoko (variant spelling Massoko, as used by the German colonial administration) and known locally as Lake Kisiba [17]. *Astatotilapia calliptera* from Lake Masoko/Kisiba is at an early stage of adaptive divergence where two diverging ecomorphs differ in body shape, diet, trophic morphology and body coloration (figure 1*b*) making it also an ideal system to study the early stages of speciation. Importantly, *A. calliptera* has a high-quality reference genome and is amenable to the laboratory environment. They have an 8–12 month generation time, breeding readily in a non-seasonal fashion allowing for year-round egg collection for gene editing and embryonic developmental studies.

We chose to generate mutants for the relatively well-characterized gene *oculocutaneous albinism type II* (*oca2*) because it is has a readily visible phenotype where black pigment production—melanin—is impaired, giving a readily assessed external phenotype from early embryo stages onwards which

facilitates quantification of editing [18,19]. *Oca2* encodes a melanosomal transmembrane protein associated with the intracellular trafficking of tyrosinase, a rate-limiting enzyme in the melanin biosynthesis pathway. *Oca2* has been associated with the evolution of amelanism and albinism in natural populations in multiple vertebrate species, such as humans, snakes, cavefish and cichlids [20–24].

In ray-finned fishes, pigmentation patterns are generated by the different number, combinations and arrangement of pigment cells: such as black melanophores, yellow to red xanthophores and reflecting silvery iridophores [25]. All pigment cell classes share an embryonic origin, deriving from the neural crest cell population during early development. Pigmentation patterning has been extensively studied in zebrafish, where the adult pigment pattern emerges through the migration and interaction between pigment cells, as well as interactions between pigment cells and the tissue environment [26–28]. *Oca2* knock-out in zebrafish is known to impair melanin production, melanophore differentiation and survival, as well as increasing the abundance of iridophores, though xanthophore- and iridophore-based stripes still form in the adult [18]. Importantly, *oca2* mutants are viable, making *oca2* single-guide RNA (sgRNA) microinjections an ideal tool to assess rates of mutagenesis and germline transmission, and to establish CRISPR/Cas9 protocols in *A. calliptera*.

CRISPR/Cas9 editing tools have revolutionized gene function analysis in a multitude of non-model species. This is due to the simplicity of the system, which requires only Watson–Crick base pairing between a sgRNA and its target sequence. The Cas9 protein will form a complex with the sgRNA, which will recognize and bind to its target sequence. The Cas9 protein will then induce a double-stranded DNA break. When double-stranded breaks are formed, the intrinsic cellular repair machinery will put the two back together either using non-homologous end joining (NHEJ) or homology-directed repair (HDR). NHEJ is an imprecise mechanism that generates small insertions or deletions that result in a frameshift. This method has been widely used to induce frameshift mutations in coding protein sequences leading to the loss of function alleles in many model systems including other cichlids [13,29–35]. HDR on the other hand uses a DNA template to guide the repair, thus by providing a single-stranded DNA (ssDNA) template, one can either insert a sequence of interest (e.g. allelic exchange) or generate larger and more precise deletions [36–39].

Here, CRISPR/Cas9-mediated knock-out was employed using these two approaches—NHEJ and HDR—to respectively target coding and non-coding regions. First, exons 1 and 3 of the *oca2*-coding sequence were targeted with sgRNAs with the intent of generating frameshift coding mutations. Second, an HDR ssRNA template was used to generate an approximately 1100 bp deletion in the 3′ untranslated region (UTR) of *oca2*. More specifically, two sgRNA target sequences were identified—one at either end of an approximately 1100 bp region in the 3′ UTR. These were then co-injected with a 100 bp ssDNA template that was mutually homologous to 50 bp at either target site. This ssDNA template facilitates HDR to replace the region in between the target sites with a deletion [39].

Using these two approaches, we generated coding and non-coding *oca2 A. calliptera* mutants using site-directed disruption with CRISPR/Cas9. As expected, the loss of *oca2* function results in amelanism due to the inability to synthesize melanin. The deletion in the 3′ UTR region yielded no visible phenotypic effect. Coding and non-coding mutations were successfully transmitted to the next generation. The establishment of CRISPR/Cas9 methodologies in *A. calliptera* provides a platform for the future analysis of coding and regulatory variation in one of the most astonishing vertebrate adaptive radiations—Malawi cichlid fishes—and will enhance our understanding of the genomic basis of organismal diversity.

2. Methods

2.1. Fish maintenance and crossing

Astatotilapia calliptera were kept under constant conditions (28 ± 1°C, 12 h dark/light cycle, pH 8) in 220 l tanks. All animals were handled in strict accordance with the protocols listed in the Home Office project licence PCA5E9695. Fish were fed twice a day with cichlid flakes and pellets (Vitalis). Tank environment was enriched with plastic plants and hiding tubes, and tank bottoms were covered with sand. Males were provided with a clay pot in which they established a territory and spawned with gravid females. Males and females were housed in the same tank but separated by a divider to control the timing of spawning. Males were housed singly, while females were kept in groups of 8–15 females. On the day of spawning, the divider was removed, and interactions were

monitored for spawning. If spawning was detected, the fish were given an additional 30–60 min to fertilize the eggs. The fertilized eggs were then removed from the female's buccal cavity and injected with sgRNAs and Cas9 protein.

2.2. sgRNA design and synthesis

CRISPR/Cas9 targets were selected with the CHOPCHOP software online (http://chopchop.cbu.uib.no/) using the *Astatotilapia burtoni* genome as a reference. Basic local alignment search tool [40] was then performed with the *A. calliptera* genome at Ensembl to confirm homology and avoid off-targets. sgRNAs used in this study start with GG or GA followed by N18, which are directly upstream of the NGG PAM sequence (5′-GG-N18-NGG-3′ or 5′-GA-N18-NGG-3′) to satisfy the requirements for *in vitro* transcription using a T7 or SP6 promoter, respectively. We designed three sgRNA in exon 1 (GACGGCATCCCAAGGCCACC, GGTCACCGAAGGCGGTGGCA and GGGGAACTATGTCTGCTG GA), one sgRNA in exon 3 (GAACAACGGCTCCCTGGACG) and two sgRNA in the 3′ UTR region (GAGTGGTCACACAGTTTCTT and GATCAACTAACGATTGATTA) (figures 2 and 3). The PCR primers for sgRNA synthesis are given in electronic supplementary material, File S1, table S1. To synthesize sgRNAs, we used the cloning-free method described in Varshney *et al*. [41] using T7 or SP6 polymerases (NEB) depending on the 5′ sgRNA sequence [41]. The sgRNAs were purified using the Qiagen RNeasy kit.

2.3. Microinjection

After collection eggs were placed into wells created by a mould with circular indentations in 2% agarose made with tank water (see Li *et al*. [35] for more information on the mould). Single-cell embryos were injected with a mixture of sgRNAs at 300 ng μl^{-1} each, together with True Cut Cas9 Protein V2 (Invitrogen) at 150 ng μl^{-1} and dextran labelled with TexasRed (ThermoFisher Scientific, 10 000 MW) at 0.25%. Three injection mixes were used: (i) sgRNA1 and sgRNA2 targeting exons 1 and 3; (ii) sgRNA3 and sgRNA4 targeting exon 1; or (iii) sgRNAUTR1 + sgRNAUTR2. To improve deletion efficiency, a 100 bp ssDNA (IDT Technologies) with left and right homology arms (figure 3*a*) located at the outer sides of the Cas9 cutting sites was used at 20 ng μl^{-1}. Microinjection needles were pulled manually from glass capillaries (GC100F-10, 1.0 mm O.D, 0.58 mm I.D, Harvard Apparatus) using a Sutter P-97. Needles were opened by gently tapping the needle on a Kimwipe to break the tip to a diameter of approximately 10 µm diameter. Each egg was injected using a pulse-flow nitrogen injection system (MPPI-3 with a back pressure unit) with two pulses at 1 ms and 40 psi (approx. 1–2 nl). The injected embryos were kept individually in 6-well plates, in an orbital shaker at 25°C in the presence of methylene blue (10 mg ml^{-1}) and with daily water changes.

2.4. Germline transmission rates and F1 progeny genotyping of *oca2*-coding mutants

Four mosaic oca2 male mutants were reared until adulthood and crossed with wild-type females (table 2). Germline transmission rates were quantified by genotyping potential F1 heterozygotes. DNA was extracted from 6 to 14 dpf embryos (after yolk removal) using the DNA miniprep kit (Zymo). PCR products were amplified with Phusion (NEB), following the manufacturer's specifications, with an annealing temperature of 62°C. Primer sequences for exon 1 and exon 3 genotyping are listed in the electronic supplementary material, table S2. PCR products were purified with QIAquick PCR Purification Kit (Qiagen). The presence of heterozygous mutants was then confirmed using Sanger sequencing. Sequence analysis was performed using the Synthego ICE CRISPR analysis tool (https://ice.synthego.com/). This tool infers CRISPR edit sites from sequences derived from heterozygous or mosaic individuals. A summary of the analysis of Sanger sequencing fragments is detailed in the electronic supplementary material, File S2. Sequence traces were analysed on Geneious Prime to detect sequence quality drops associated with the sgRNA cutting site. Further, mutant sequences were extracted using the ICE CRISPR analysis tool by selecting the most frequent mutant allele and aligned with the MAFFT alignment plugin on Geneious Prime (figure 2*b–d*). Two *oca2* mosaic coding mutant females were incrossed with one *oca2* mosaic male to generate F1s with two oca2 mutant alleles. Germline transmission was inferred by visual quantification of the number of embryos lacking melanic pigmentation. These estimates probably represent an underestimation of transmission rates, since heterozygotes do not present an amelanistic phenotype.

2.5. Germline transmission rates and F1 progeny genotyping of *oca2* 3′ untranslated region deletion mutants

G0 mosaics and F1 heterozygous mutant progeny were assessed by PCR using two primers flanking the cutting sites. The forward primer is located 207 bp upstream of the left cutting site and the reverse is 400 bp downstream of the right cutting site (electronic supplementary material, File S1, table S2). This assay differentiates between the wild-type individuals and individuals carrying the desired deletion. PCR on wild-type individuals results in only one PCR fragment, whereas mosaic individuals carrying the deletion will show two fragments—the wild-type sequence (approx. 1715 bp) and the sequence containing the deletion (approx. 624 bp). Only one G0 individual tested positive for the deletion. This G0 individual was crossed with wild-type females (table 4). DNA was extracted from a fin clip of the G0 founder and from 8 dpf F1 embryos (after yolk removal). PCR was performed with OneTaq (NEB), following the manufacturer's specifications, with an annealing temperature of 60°C. PCR purification of the deletion fragments was performed with QIAquick Gel Extraction Kit (Qiagen). The presence of the deletion in the G0 and F1 individuals was then confirmed using Sanger sequencing. Sequences were aligned using the MAFFT alignment plugin on Geneious Prime (figure 3*b*).

2.6. Embryo and adult imaging

Embryos were imaged on a Leica M205 FCA stereoscope with a DFC7000T camera under reflected light darkfield. For each embryo, images were taken at multiple focal distances. These images were then focus-stacked using Helicon Focus or Photoshop to produce a single image with all cells in focus. To prevent movement between imaging different focal planes, post-hatching embryos were anaesthetized by submersion in 0.02% Tricaine methanesulphonate (Sigma-Aldrich E10521) for the duration of imaging (approx. 2 min per embryo) with the yolk supported in a shallow well of solidified 1% low-melting agarose (Promega, V2111). Adult fish were photographed using a Panasonic DMC GX7 camera with a Panasonic Lumix G 20 mm pancake lens, in a photography tank containing a scale. Lighting conditions were standardized using two light sources, one either side of the camera and a grey background.

3. Results

3.1. Site-directed disruption of *Astatotilapia calliptera oca2*-coding sequence

To demonstrate the feasibility of genome editing in *A. calliptera*, we generated mutations in the coding sequence of *oca2*. Two injection mixes were used, each containing two sgRNAs with the intent to increase the chances of introducing mutation [35]. These were co-injected with Cas9 protein into fertilized single-cell eggs (figure 2*a*). The first mix contained sgRNA 1 and sgRNA 2, targeting exon 1 and exon 3 respectively (figure 2*a*). The second contained sgRNA 3 and sgRNA 4 both targeting exon 1 (figure 2*a*). Exons near the 5′ end of the gene were selected to increase the chance of a frameshift mutation causing a missense translation for most of the length of the protein sequence. Embryos were screened at 4 days post-fertilization (dpf, 25°C) when the retinal pigment epithelium becomes pigmented with melanin. Both injection mixes yielded mosaic individuals with an average survival rate of 28.5%. The percentage of mosaic individuals was variable ranging from 18% to 100% with an average of 60% (table 1).

To investigate if mutations could be transmitted to the following generations, fish showing mosaic phenotypes were raised to adulthood. From these G0 adult fish, four males were crossed with WT females. In addition, we incrossed one *oca2* mosaic male with two *oca2* mosaic females to obtain *oca2* mutants carrying two *oca2*-coding knock-out alleles and hence with a visible amelanistic phenotype in one generation (table 2). The genotyping of sequencing products derived from the progeny of crosses of male founder individuals with wild-type females showed an average transmission rate of 47% (table 2). The lowest transmission rate (none) was detected in a male with low levels of phenotypic amelanistic mosaicism, whereas transmission was highly effective for the other three mosaic males with extensive amelanism (33–78%). As germline transmission was high, we were able to generate two incrosses between *oca2* mosaic mutants that both generated amelanistic phenotypes. One of the incrosses generated 10 embryos all with amelanistic phenotypes. Since this mutation is recessive, this result indicates that both progenitors exhibited a transmission rate of 100% for this clutch, generating

Table 1. Percentage of *oca2* mosaic individuals induced by CRISPR/Cas9 in G0s.

target	injected	survived	survival (%)	mutant	mosaic frequency (%)
#1 *oca2* exon 1 & 3	36	17	47	17	100
#2 *oca2* exon 1	35	7	20	4	57
#3 *oca2* exon 1	53	11	21	2	18
#4 *oca2* exon 1	25	9	36	4	44
#5 *oca2* exon 1	55	15	27	6	40
#6 *oca2* exon 1	20	4	20	4	100
		average survival	28.5	average mosaicism	60

Table 2. Germline transmission of six founder crosses for the *oca2* loss of function mutations.

group	founder cross	#F1s tested	positive individuals	germline transmission (%)
oca2 mosaic male × WT females: germline transmission quantified by PCR genotyping				
#1 *oca2* exon 1	*oca2*♂^{1} × wt♀	9	7	78
#2 *oca2* exon 1 & 3	*oca2*♂^{2} × wt♀	9	0	0
#3 *oca2* exon 1 & 3	*oca2*♂^{3} × wt♀	9	7	78
#4 *oca2* exon 1 & 3	*oca2*♂^{4} × wt♀	9	3	33
			average transmission	47
oca2 mosaic × *oca2* mosaic: germline transmission quantified by presence of amelanistic individuals				
#5 *oca2* exon 1	*oca2*♂^{5} × *oca2*♀^{1}	10	10	100
#6 *oca2* exon 1	*oca2*♂^{5} × *oca2*♀^{2}	10	2	20
			average transmission	60

progeny carrying two *oca2*-coding knock-out alleles. The second incross generated 10 embryos with only two showing the amelanistic phenotype, which implies a rate of 20% transmission for one of the progenitors. Taken together, germline transmission was high and observed in all crosses where founders showed high levels of phenotypic amelanistic mosaicism (table 2).

Sequence analysis of the F1 progeny resulting from crosses #1, #3 and #4 (table 2) showed that both injection mixes resulted in deletions of variable sizes ranging from 1 bp to 21 bp deletions (figure 2*b–d*). The genotyping of F1 progeny from crosses #3 and #4, resulting from microinjections using sgRNA1 and sgRNA2, which, respectively, target exon 1 and exon 3 (figure 2*b*,*c*), showed that these two guides have different germline transmission rates, with sgRNA1 presenting a higher frequency (67% for #3 and 33% #4) than sgRNA2 (44% for #3 and 22% for #4) (electronic supplementary material, File S2). For cross #3, the transmission rates for each individual guide were lower than the calculated rate for when the two are combined (table 2, crosses #3 and #4), showcasing the benefits of injecting several guides in combination. This is further strengthened by the genotyping results from cross #1, which showed that only one of the two guides injected resulted in indels (sgRNA 4, figure 2*d*).

3.2. Deletion of *Astatotilapia calliptera oca2* 3′ untranslated region

The majority of a given organismal genome is non-coding in nature and regulates the timing and location of gene expression and transcript stability. It has been repeatedly shown that non-coding sequence divergence contributes greatly to cichlid diversity [13,15,42–44]. For example, the comparison of the first five cichlid reference genomes showed an abundance of non-coding element divergence and

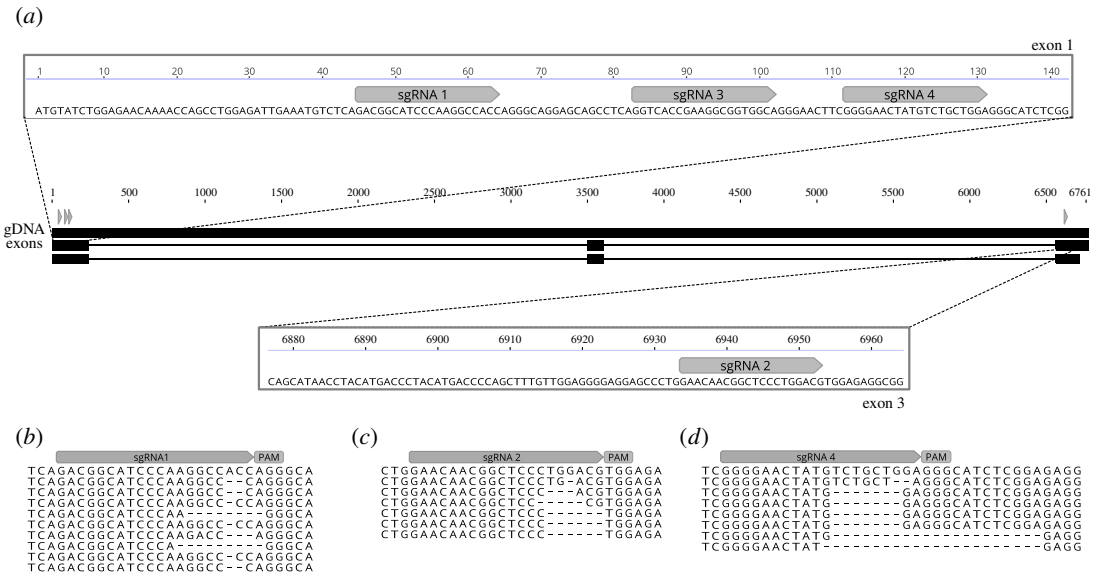

Figure 2. Efficient indel generation of *oca2*-coding sequence by CRISPR/Cas9. (*a*) Four sgRNAs were designed to cut the genomic sequence at exon 1 and exon 3. Two injection mixes were used, one containing sgRNA1 and sgRNA2 targeting exon 1 and exon 3, and the other containing sgRNA3 + sgRNA4 both targeting exon 1. Alignment of mutant F1 individuals derived from crosses #1, #3 and #4 are shown for (*b*) sgRNA1, (*c*) sgRNA2 and (*d*) sgRNA4. All F1 individuals were wild-type at the cutting site of sgRNA3.

found that transposable element insertions upstream of transcription start sites were associated with expression divergence [15]. Further, 3′ UTRs also act as key regulators of gene expression, containing binding sites for microRNAs and RNA-binding proteins [45]. The investigation of cichlid microRNA genes detected signatures of divergent natural selection in microRNA target sites among Lake Malawi cichlids [44]. A comparative transcriptome analysis has further revealed little divergence at protein-coding sequences, but a high diversity in UTRs [43]. Taken together, these studies suggest that regulatory evolution plays a key role in cichlid diversification. Thus, it is important to establish a protocol that allows for testing of the function of non-coding regions associated with trait variation. For this purpose, we took advantage of the HDR CRISPR/Cas9 method to generate a large deletion in the 3′ UTR region of *oca2*.

First, two sgRNA target sequences were identified—one at either end of a 1096 bp region (figure 3*a*). Then, a 100 bp ssDNA repair template was designed to be homologous to the flanking regions of each target site (50 bp upstream and 50 bp downstream), in order to mimic a deletion when compared with the wild-type sequence (figure 3*a*). A mix of the two sgRNAs, the ssDNA together with Cas9 protein was microinjected into fertilized single-cell eggs (electronic supplementary material, File S1, table S1). As there was no observable phenotype, the number of mosaic 3′ UTR deletion mutants was assessed by PCR and Sanger sequencing using two primers flanking the cutting sites (207 bp upstream of the left cutting site and 400 bp downstream of the right cutting site) (electronic supplementary material, File S1, table S2). This assay can differentiate between the wild-type individuals and individuals carrying the desired deletion: PCR on wild-type individuals would result in only one PCR fragment, whereas mosaic individuals carrying the deletion would show two fragments—the wild-type sequence (approx. 1715 bp) and the sequence containing the deletion (approx. 624 bp). Using this assay, we determined that the percentage of mosaic individuals was 25% and 0% in the two clutches injected, with the presence of only one positive mosaic mutant (table 3).

To determine if deletions are transmitted to the following generations, the G0 mosaic individual for the deletion was raised to adulthood. This *oca2* 3′ UTR mosaic male mutant was crossed with wild-type individuals and showed a germline transmission of 38% (table 4). We genotyped F1s deriving from this cross and confirmed the presence of germline transmission for the deletion. Sequencing of G0 and F1 individuals further confirmed the presence of deletions between the two target sites. The G0 founder showed the presence of a deletion and 5 out of 13 F1s inherited mutations (figure 3*b*). While two of the F1s (F1_#1 and F1_#8) had a precise deletion, the other three showed the deletion (F1_#5, F1_#7 and F1_#13) followed by an approximately 100 bp downstream insertion (figure 3*b*). This insertion showed homology to the HDR template which was potentially inserted—knocked-in—as part of the

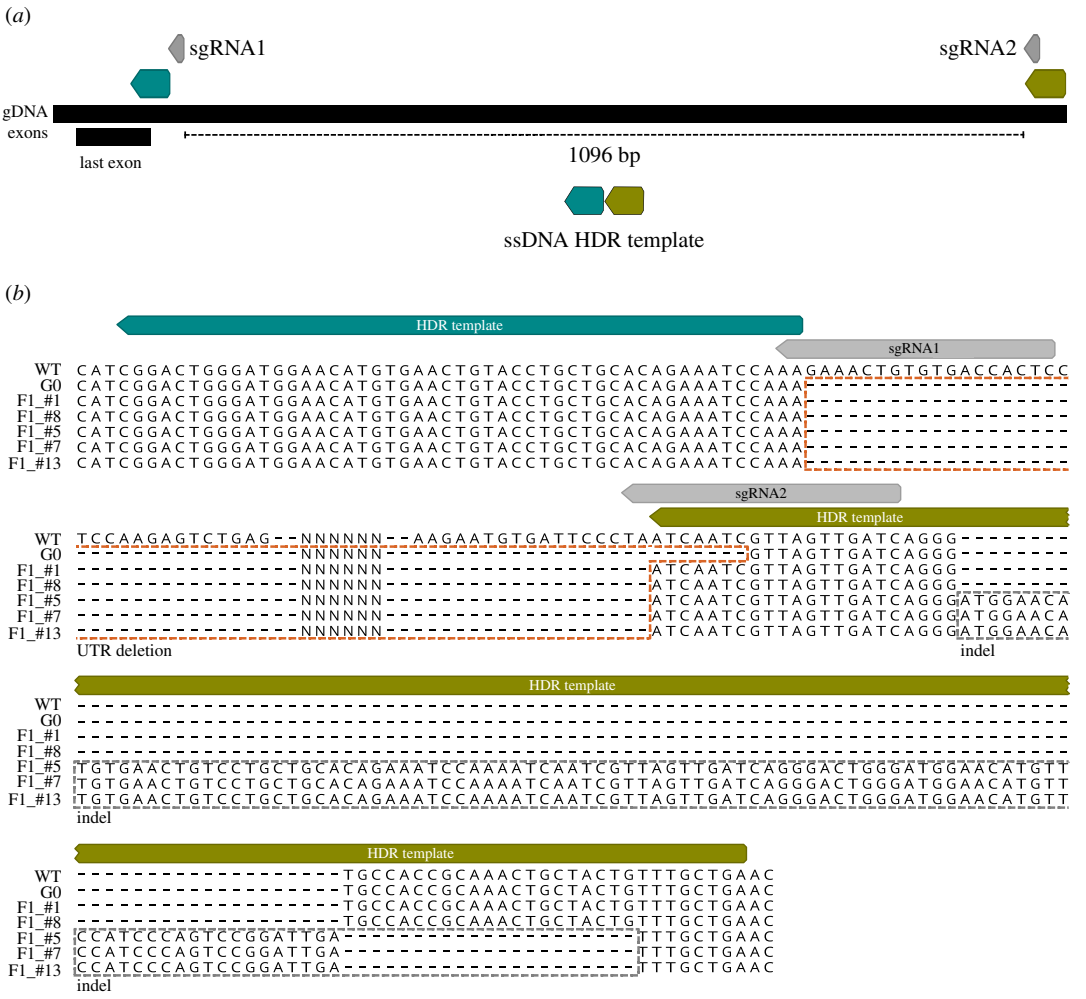

Figure 3. Large deletion of *oca2* 3′ UTR sequence (approx. 1096 bp) using one pair of sgRNAs (grey boxes) and one ssDNA HDR template. (*a*) A single-stranded HDR template with 50 bp left and right homology arms (blue and green boxes, respectively) were co-injected with two sgRNAs flanking the desired deletion sites. (*b*) Sequencing of the PCR products confirmed the deletion in the G0 and F1s. The 3′ UTR deletion is marked with an orange dashed box. In three of the F1s (#5, #7 and #13), the deletion is followed by a downstream indel marked with a grey dashed box.

repair mechanism (electronic supplementary material, figure S1). These results show that the deletion of large non-coding fragments was successful in *A. calliptera*, but careful screening and sequencing of F1s is required to confirm the precise nature of the deletions. The injection of different sgRNA and HDR template combinations, using larger clutches and screening more F1s will contribute to the refinement of this technique.

3.3. Phenotype of *oca2*-coding and non-coding mutants in *Astatotilapia calliptera*

In agreement with previous work in other model systems, *oca2* loss of function mutations led to a reduction in melanic pigmentation. In wild-type embryos, yolk melanophores are the first visible pigment cells to appear on the embryo (figure 4*a*), and they remain on the yolk until body wall closure. As such, the first observed phenotype in embryos injected with sgRNAs targeting the *oca2*-coding sequence was a reduction in visible yolk melanophore abundance at 4 days post-fertilization (dpf) (figure 4*b*). In F1 fish with two *oca2* mutant alleles, there was a complete lack of pigmented melanophores at this stage (figure 4*c*); this amelanistic phenotype persisted throughout development.

By 10 dpf the degree of melanic coverage along the body increases in wild-type larvae, particularly in the head region, where the yolk melanophores increase in number and are more densely packed. The retina becomes fully pigmented, containing both melanin and iridophores (figure 4*d*). On the contrary, *oca2* mosaic mutant larvae continued to have fewer visible melanophores appearing on either the head

Table 3. Percentage of *oca2* 3′ UTR mosaic mutants induced by CRISPR/Cas9 in G0s.

target	injected	survived	survival (%)	mutant	mosaic frequency (%)
#1 *oca2* 3′ UTR	20	4	20	1	25
#2 *oca2* 3′ UTR	58	3	5	0	0
		average survival	12.5	average mosaicism	12.5

Table 4. Germline transmission of one founder cross for the *oca2* 3′ UTR deletion.

group	founder cross	#F1s tested	positive individuals	germline transmission (%)
#1 *oca2* 3′ UTR	*oca2 utr* ♂^{6} × wt ♀	13	5	38

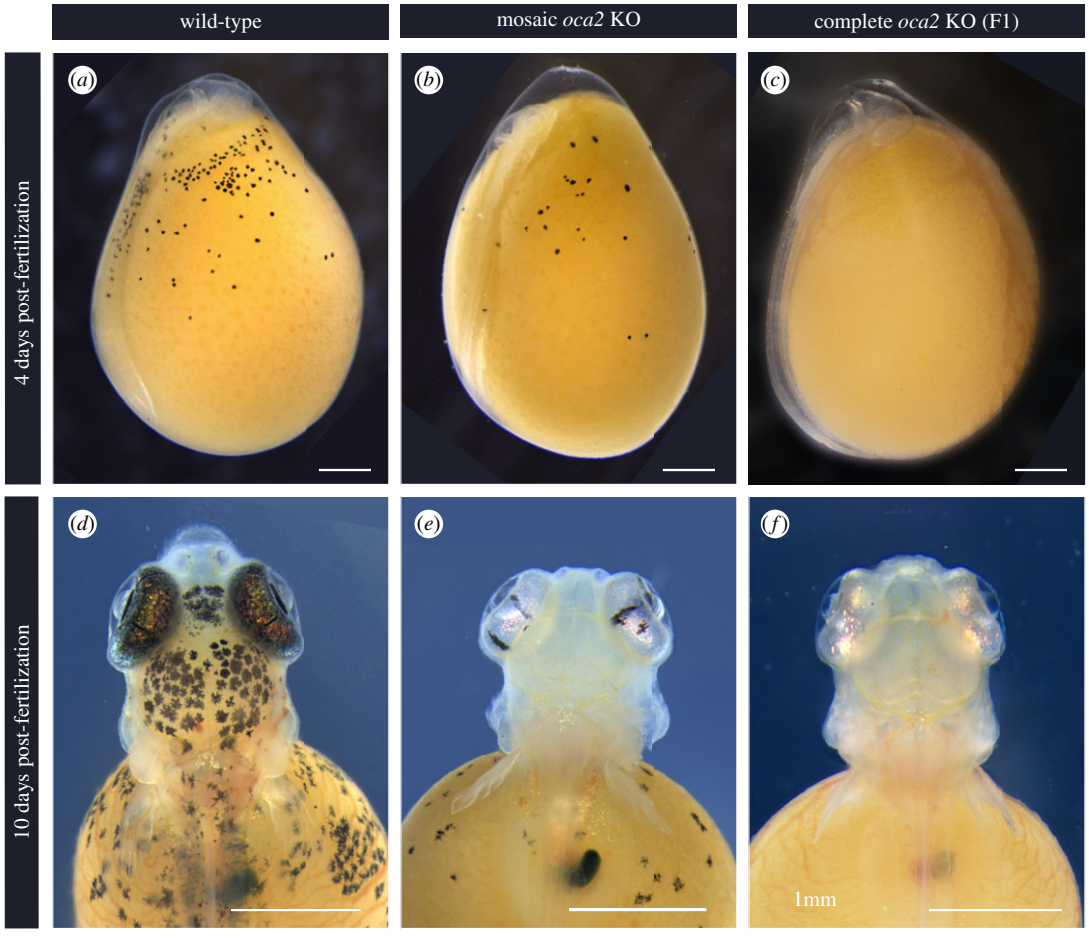

Figure 4. *Oca2* loss of function embryonic phenotypes (25°C). (*a–c*) Embryo development at 4 days post-fertilization and (*d–f*) 10 days post-fertilization for wild-type (*a,d*), mosaic G0 (*b,e*) and F1 *oca2*-coding knock-out embryos (*c,f*). Scale bar 1 mm.

or on the yolk (figure 4*e*) and none in F1 fish with two mutant alleles (figure 4*f*). Despite the lack of melanin pigment, the retinae of *oca2* mutant larvae were bright and iridescent indicating the presence of iridophores (figure 4*e,f*).

Throughout all the stages of development described, there was no apparent difference in phenotype between wild-type embryos and the *oca2* 3′ UTR deletion mosaic (electronic supplementary material, File

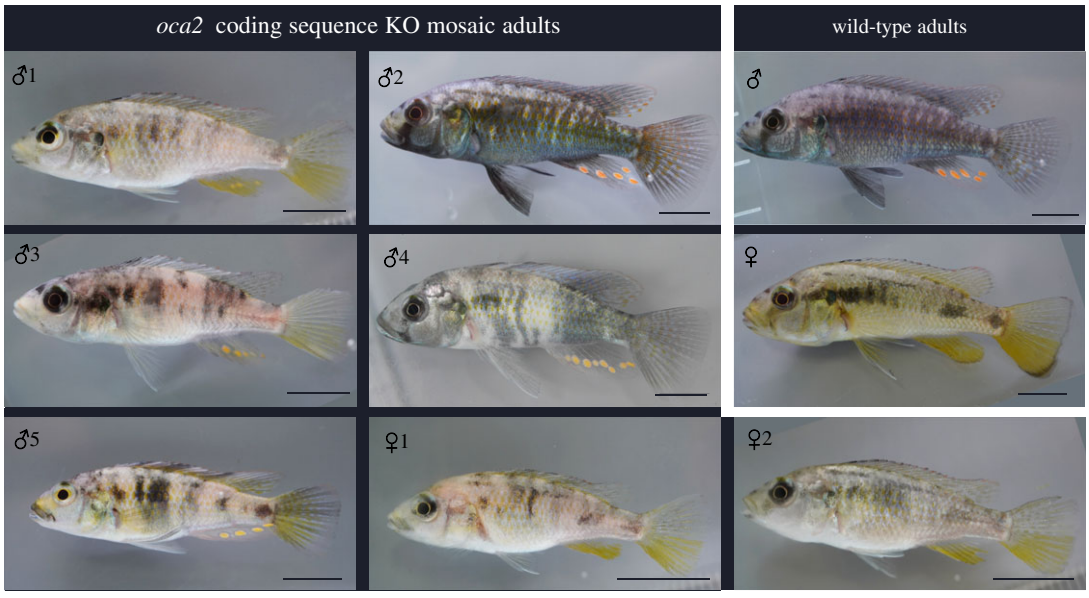

Figure 5. *Oca2*-coding sequence G0 adult phenotypes. Mosaic injected *oca2*-coding region knock-outs compared with wild-type adults. Individual numbering corresponds to table 2. Scale bar 1 cm.

S1, figure S2). Both male and female mosaic *oca2*-coding knock-out mutants continued to display a hypopigmented phenotype as adults (figure 5), while the mosaic *oca2* 3′ UTR deletion mutant had a wild-type phenotype (electronic supplementary material, File S1, figure S3). This result has to be taken with caution as only one G0 individual tested positive for the deletion (table 3) and may carry very few cells with biallelic mutations. The generation of homozygous mutants would be required to fully comprehend the phenotypic effects of the 3′ UTR deletion.

F1 adult fish with two *oca2*-coding knock-out alleles had a typical amelanistic phenotype, with a complete absence of black pigmentation and red retina (figure 6). These are often used as diagnostic criteria for albinism; however, we refer to this phenotype as amelanism because a strict definition of albinism requires a lack of all pigments [23]. In vertebrate taxa where the only pigment cell type is melanocytes (mammals and birds), amelanistic individuals are albinistic. In vertebrates with multiple cell types, loss of pigments from xanthophores would additionally be required to describe an individual as albino. The amelanistic adult *A. calliptera* had yellow and red pigmentation and therefore does not meet the strict definition of albinism [23].

We compared the pigmentation patterns with the siblings of amelanistics: as the offspring of a cross between two mosaic mutant fish, these siblings may either be homozygous wild-type or heterozygous for the *oca2*-coding knock-out which also has a wild-type phenotype [18]. In amelanistic adults, black pigmentation patterns on the body and fins were absent, which includes the faint vertical bars on the trunk (figure 6*a*,*b*), solid black patch on the operculum (figure 6*c*,*d*), the black bar across the eye in males (figure 6*c*,*d*), the skin throughout the trunk (figure 6*e*,*f*), the anterior of the dorsal fin (figure 6*g*,*h*), and the base, spines and edges of the caudal fin (figure 6*i*,*j*). In the amelanistic mutants, there was greater yellow/orange pigmentation visible across the whole body. Areas that are exclusively black in wild-type were instead bright and reflective in the amelanistic individuals. The close-up pattern on the body of alternating light and dark patches was maintained in amelanistic adults (figure 6*e*,*f*). Interestingly, in this pattern, the blue regions of the wild-type appeared white in the amelanistic, and red erythrophores present in the amelanistic individuals were not visible in the wild-type (figure 6*e*,*f*).

4. Discussion

Mapping genotypic variation to phenotypic variation is one of the major goals of evolutionary biology. Hence, a multitude of candidate loci underlying adaptive trait variation have been identified in a wide range of organisms [46]. Most of these studies are performed in species harbouring natural variation but that are typically considered non-model systems due to the lack of tractable genetic tools. The recent

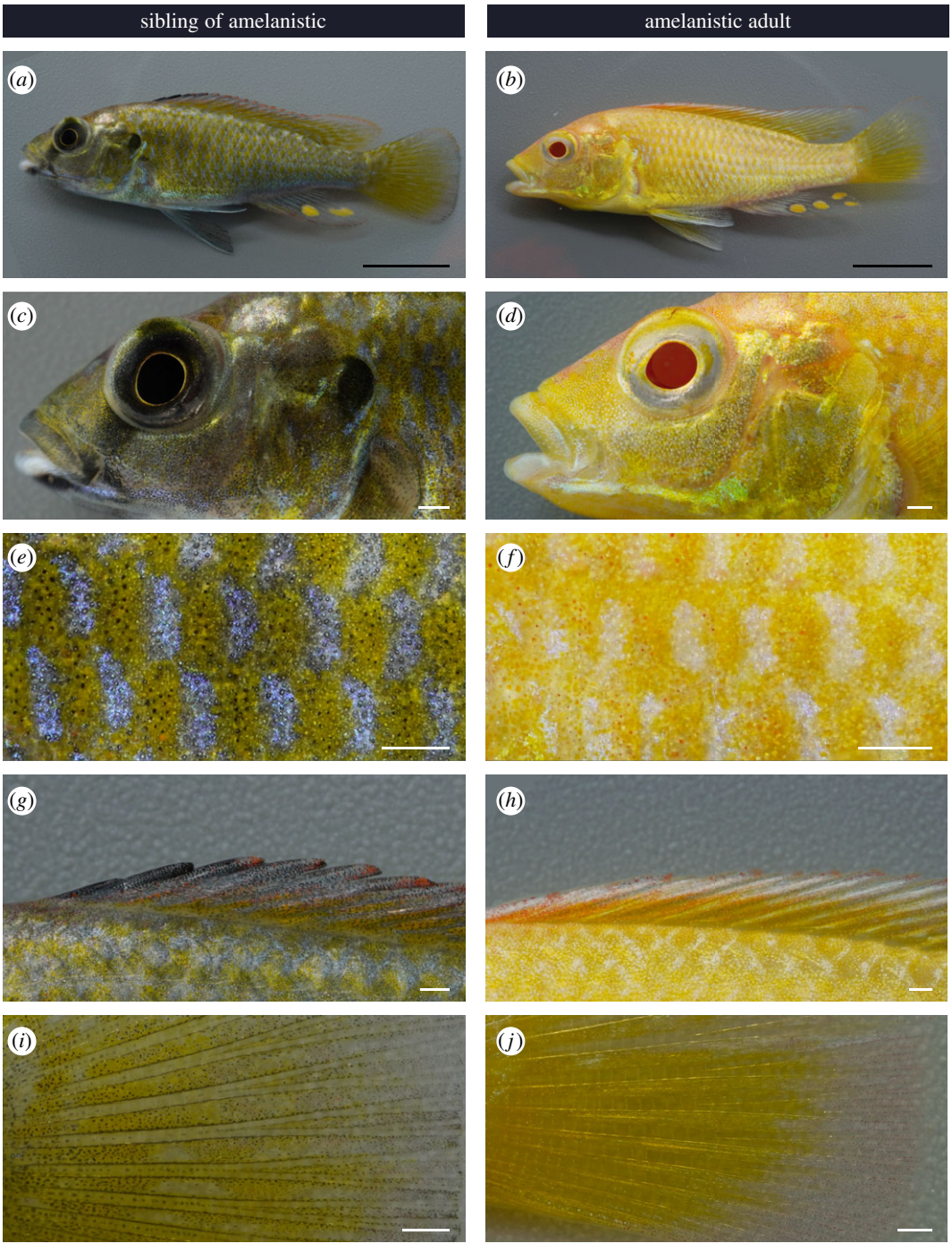

Figure 6. *Oca2* amelanistic phenotype of adults. Comparison of F1s with wild-type and amelanistic appearance. (*a,b*) full body, (*c,d*) head, (*e,f*) close-up of anterior trunk, (*g,h*) dorsal fin anterior and (*i,j*) caudal fin close-up of central spines, base of fin to the left and distal edge at the right. Scale bars 1 cm for (*a,b*) and 1 mm for (*c–j*).

development of genome editing tools such as CRISPR/Cas9 is thus revolutionizing the field of evolutionary biology, allowing for candidate gene function tests in virtually any organism and uncovering the genomic and developmental basis of adaptation and diversification. In this study, we adapted existing protocols to establish CRISPR/Cas9 genome editing in the cichlid fish *Astatotilapia calliptera*. We generated both coding and non-coding mutations in *oca2* that were efficiently transmitted through the germline to the next generation. To our knowledge, this is the first report of successful genome editing in this species or any cichlid within the Malawi radiation, and as such, represents the first step towards testing the genes and regulatory elements underlying variation in the Malawi cichlid radiation.

The amelanistic phenotype of *oca2* is expected given the role of *oca2* in tyrosinase transport for melanin production and melanosome maturation in melanophores [18,47,48]. This demonstrates that *oca2* is a useful gene to target for establishing and refining CRISPR/Cas9 editing in a new species: it is easy to screen for mutations as with other melanin synthesis pathway genes [35]. Similarly to *tyrosinase* knock-outs in the Lake Tanganyika cichlid *A. burtoni* [35], this *oca2* mutant line would permit unobstructed imaging of subdermal structures and fluorophores *in situ* during embryo development, enabling interspecific comparisons for such studies.

Despite the lack of melanin, typical colour patterns are still noticeable on amelanistic *A. calliptera*. As teleost fish colour patterns self-organize through interaction between different pigment cells, this suggests that unpigmented melanophores are still present and contributing to pattern formation [49]. However, *oca2*-deficient zebrafish also show an increase in iridophore numbers suggesting that the loss of *oca2* could affect other pigment cells [18]. We consider both of these possibilities when interpreting the amelanistic coloration phenotype. For example, the switch from blue to white reflective coloration in the alternating patches on the trunk indicates that the presence of black pigment is required for blue coloration in *A. calliptera* (figure 6). This may act via an influence of pigmented melanophores on iridophores. Different arrangements and spacing of the reflective platelets in iridophores change the observed colour between white and blue [50] and in zebrafish melanophores may induce iridophores to change shape and colour from white and dense to blue and loose [51]. Similarly, the greater visible yellow/orange coloration due to xanthophores, red erythrophores and bright reflective patches of iridophores in amelanistics could be due to melanin obscuring this pigmentation in wild-types (figure 6). In some cichlid species, superficial melanophores are found in the dermis, above the hypodermis [52] so it is possible that they cover other pigment cells in *A. calliptera*. Alternatively, there may be greater numbers of these cell types in the amelanistic individuals. Comparison of the number and type of pigment cells during wild-type and amelanistic development may provide initial insights into chromatophore interactions in cichlids.

Here, we targeted coding and non-coding *oca2* sequences demonstrating that despite low embryonic survival, mosaic mutants and germline transmission occurs at an efficient rate. Embryo survival was low, averaging 20%, with most deaths occurring due to perforation of the yolk and its subsequent leakage. This low survival is comparable to the microinjection survival rates observed in other cichlids (20% in *Oreochromis niloticus* and 30% in *A. burtoni*) [32,35]. Despite the low survival, mosaic mutant generation occurred at a high rate. Mosaic frequency was higher for coding sequence mutants (approx. 50%) than for the non-coding deletion mutants (approx. 12.5%). This probably reflects the lower efficiency of the HDR mechanism compared with NHEJ [53]. Alternatively, this result may also reflect locus-dependent differences in mutation rate. To distinguish between the two hypotheses, a comparison between HDR and NHEJ modifications at the same locus is required. Nonetheless, we observed transmission of mutations to the next generation in both cases. *Astatotilapia calliptera* species reach maturity on average at 8 months at which point they usually lay on average approximately 20 eggs, with clutch size increasing with age and size [16]. Despite low survival and low clutch sizes at young ages, germline transmission is high and as such it is possible to establish a breeding population of stable mutant *A. calliptera* within 16 months. One possibility to increase spawning frequency and increase clutch sizes to maximize the number of mutants, is peritoneal injections of Ovaprim, a commercially available mixture of gonadotropin-releasing hormone analogue and a dopamine receptor antagonist. Such injections resulted in a reduction in spawning interval by 5 days and a twofold increase in egg yield in *A. burtoni* [35]. A similar effect would be expected in *A. calliptera*.

As 3′ UTRs act as key regulators of gene expression, and there is evidence for high diversity in UTRs among Malawi cichlids, we decided to establish a protocol to induce large deletions in the 3′ UTR of *oca2*. We were able to verify successful deletion of an approximately 1100 bp stretch of the *oca2* 3′ UTR via HDR. However, while we could detect precise deletions in the G0 mutant and in two F1 individuals, some F1 progeny also contained an approximately 100 bp indel. This insertion was probably the result of erroneous integration of fragments of the HDR template, as some regions shared homology with the template but in random orientations. Erroneous integration of HDR template fragments has been reported in CRISPR/Cas9-mediated HDR in other species including zebrafish, in which frequency of template integration was found to influence overall knock-in efficiency [54]. In future applications, refinement of HDR template composition and chemical impairment of the NHEJ pathway may improve HDR efficiency in *A. calliptera* [55]. There were no apparent phenotypic differences between the UTR deletion mosaic individual and wild-types, consistent with the expectation that the effects of *cis*-regulatory mutations may be less severe than coding sequence mutations. Further examination of the phenotypic effects of the *oca2* 3′ UTR deletion will require generating homozygous mutants.

Genome editing in this species is particularly relevant on many fronts. First, this species is highly diverse, inhabiting a range of habitats (lacustrine and riverine) and showing extensive populational variation in several morphological, physiological and life-history traits [16]. *Astatotilapia calliptera* 'masoko' in particular is a key example of ongoing sympatric speciation, with two divergent ecomorphs differing in depth habitat and dietary preferences and many other morphological traits, such as male colour, craniofacial profile and pharyngeal jaws (figure 1*a*,*b*). These differences are associated with assortative mating and local adaptation providing a good set-up to address the early stages of adaptive diversification within the context of both natural and sexual selection. Further, there are plenty of genomic resources for this species, with a reference genome assembly at the chromosomal level and with hundreds of low coverage genomes distributed across several populations [5,56,57]. These genomic resources combined with the genome editing tools and *A. calliptera* amenability to the laboratory allows for the tackling of adaptive diversification from both the genomic and developmental point of view. Additionally, it has also been suggested that the Malawi cichlid radiation initially stemmed from a generalist *Astatotilapia*-type lineage. The approximately 850 Malawi cichlid species can be grouped into seven eco-morphological groups, resulting from three separate cichlid radiations that stemmed from a generalist *Astatotilapia*-type lineage [5,58]. The divergence started with the split of the pelagic genera *Rhamphochromis* and *Diplotaxodon*, followed by the shallow- and deep-water benthic species, as well as the utaka lineage (water column shoaling cichlids), and finally the split of mbuna (rock dwelling cichlids). The ancestor of these three radiations was, most likely, very similar to *A. calliptera*, in terms of ecology and phenotype [5]. As such, *A. calliptera* is a useful model in which to develop functional tools to explore Malawi cichlid explosive diversification.

An important attribute of Malawi cichlids is the ease of establishing interspecific crosses for genetic mapping of traits of interest. Using such an approach, several studies identified genes associated with interspecific variation in craniofacial profiles, jaw attributes, colour patterns and sex determination systems. The increase in genomic resources and the low costs of whole genome sequencing are also leading to an increase in genome-wide association studies in wild populations giving unprecedented insights into intraspecific variation [57,59]. A commonality between all these studies is that often the causal variants are in non-coding regions, hence establishing methods to edit non-coding regions will facilitate the dissection of their functional role. Here, both non-coding and coding sequence editing protocols are suited for the loss of function experiments. The next step is to establish the targeted introduction of specific mutations using a knock-in approach, whereby a genomic variant associated with variation across species can be transferred from one species to the other. This approach will provide the causative link between genotype and phenotype variation and provide a genetic and developmental mechanism as to how organismal variation emerges.

In summary, we have demonstrated the successful targeting of coding and non-coding sequences in the cichlid *A. calliptera* using CRISPR/Cas9. As the extant species of the lineage ancestral to the lake Malawi cichlid radiation, and as a very diverse species complex itself, *A. calliptera* is an ideal species with which to test hypotheses regarding speciation, adaptation and trait diversification. The establishment of genome editing tools for such key non-model species promises to reveal novel genetic and developmental mechanisms by which organismal diversity emerges.

Ethics. All animals were handled in strict accordance with the protocols listed in the Home Office project licence PCA5E9695.

Data accessibility. The datasets supporting this article have been uploaded as part of the electronic supplementary material [60].

Authors' contributions. J.E.: conceptualization, investigation, writing—original draft and writing—review and editing; B.C.: conceptualization, funding acquisition, investigation, writing—original draft and writing—review and editing; A.M.: investigation and writing—review and editing; G.F.T.: resources and writing—review and editing; A.M.S.: resources and writing—review and editing; D.J.: resources and writing—review and editing; E.A.M.: funding acquisition, resources and writing—review and editing; S.A.J.: conceptualization, supervision and writing—review and editing; M.E.S.: conceptualization, funding acquisition, investigation, supervision, writing—original draft and writing—review and editing.

All authors gave final approval for publication and agreed to be held accountable for the work performed therein.

Conflict of interest declaration. The authors declare no competing interests.

Funding. B.C. and A.M. are supported by the Wellcome Trust PhD Programme in Developmental Mechanisms (222279/Z/20/Z and 102175/Z/13/Z, respectively). E.A.M. is supported by Cancer Research UK (C13474/A18583 and C6946/A14492) and the Wellcome Trust (219475/Z/19/Z and 092096/Z/10/Z). S.A.J. is supported by the HFSP grant RGY0079/2018 and the NSF grant no. IOS-1825723. M.E.S. is supported by a NERC IRF NE/R01504X/1.

Acknowledgements. We thank the Animal Technicians and NACWO at the UBS Cichlid fish facility in Madingley (Cambridge) for the help in rearing wild-type and mutant fish and Members of the Miska lab and Morphological Evolution Lab for technical support and discussion.

References

1. Schluter D. 2000 *The ecology of adaptive radiation*. Oxford, UK: Oxford University Press. See https://search.library.wisc.edu/catalog/999914007502121.
2. Santos ME, Salzburger W. 2012 How cichlids diversify. *Science* **338**, 619–621. (doi:10.1126/science.1224818)
3. Kocher TD. 2004 Adaptive evolution and explosive speciation: the cichlid fish model. *Nat. Rev. Genet.* **5**, 288–298. (doi:10.1038/nrg1316)
4. Salzburger W. 2018 Understanding explosive diversification through cichlid fish genomics. *Nat. Rev. Genet.* **19**, 705–717. (doi:10.1038/s41576-018-0043-9)
5. Malinsky M, Svardal H, Tyers AM, Miska EA, Genner MJ, Turner GF, Durbin R. 2018 Whole-genome sequences of Malawi cichlids reveal multiple radiations interconnected by gene flow. *Nat. Ecol. Evol.* **2**, 1940–1955. (doi:10.1038/s41559-018-0717-x)
6. Ronco F *et al.* 2021 Drivers and dynamics of a massive adaptive radiation in cichlid fishes. *Nature* **589**, 76–81. (doi:10.1038/s41586-020-2930-4)
7. Powder KE, Albertson RC. 2016 Cichlid fishes as a model to understand normal and clinical craniofacial variation. *Dev. Biol.* **415**, 338–346. (doi:10.1016/j.ydbio.2015.12.018)
8. Edgley DE, Genner MJ. 2019 Adaptive diversification of the lateral line system during cichlid fish radiation. *iScience* **16**, 1–11. (doi:10.1016/j.isci.2019.05.016)
9. Sylvester JB, Rich CA, Loh YHE, van Staaden MJ, Fraser GJ, Streelman JT. 2010 Brain diversity evolves via differences in patterning. *Proc. Natl Acad. Sci. USA* **107**, 9718–9723. (doi:10.1073/pnas.1000395107)
10. Carleton KL, Dalton BE, Escobar-Camacho D, Nandamuri SP. 2016 Proximate and ultimate causes of variable visual sensitivities: insights from cichlid fish radiations. *Genesis* **54**, 299–325. (doi:10.1002/dvg.22940)
11. Roberts RB, Moore EC, Kocher TD. 2017 An allelic series at *pax7a* is associated with colour polymorphism diversity in Lake Malawi cichlid fish. *Mol. Ecol.* **26**, 2625–2639. (doi:10.1111/mec.13975)
12. Santos ME, Braasch I, Boileau N, Meyer BS, Sauteur L, Böhne A, Belting HG, Affolter M, Salzburger W. 2014 The evolution of cichlid fish egg-spots is linked with a *cis*-regulatory change. *Nat. Commun.* **5**, 5149. (doi:10.1038/ncomms6149)
13. Kratochwil CF, Liang Y, Gerwin J, Woltering JM, Urban S, Henning F, Machado-Schiaffino G, Hulsey CD, Meyer A. 2018 Agouti-related peptide 2 facilitates convergent evolution of stripe patterns across cichlid fish radiations. *Science* **362**, 457–460. (doi:10.1126/science.aao6809)
14. Svardal H, Quah FX, Malinsky M, Ngatunga BP, Miska EA, Salzburger W, Genner MJ, Turner GF, Durbin R. 2020 Ancestral hybridization facilitated species diversification in the Lake Malawi cichlid fish adaptive radiation. *Mol. Biol. Evol.* **37**, 1100–1113. (doi:10.1093/molbev/msz294)
15. Brawand D *et al.* 2014 The genomic substrate for adaptive radiation in African cichlid fish. *Nature* **513**, 375–381. (doi:10.1038/nature13726)
16. Parsons PJ, Bridle JR, Rüber L, Genner MJ. 2017 Evolutionary divergence in life history traits among populations of the Lake Malawi cichlid fish *Astatotilapia calliptera*. *Ecol. Evol.* **7**, 8488–8506. (doi:10.1002/ece3.3311.)
17. Turner G, Ngatunga BP, Genner MJ. 2019 The natural history of the satellite lakes of Lake Malawi. *EcoEvoRxiv* (doi:10.32942/osf.io/sehdq)
18. Beirl AJ, Linbo TH, Cobb MJ, Cooper CD. 2014 *oca2* regulation of chromatophore differentiation and number is cell type specific in zebrafish. *Pigment Cell Melanoma Res.* **27**, 178–189. (doi:10.1111/pcmr.12205)
19. Klaassen H, Wang Y, Adamski K, Rohner N, Kowalko JE. 2018 CRISPR mutagenesis confirms the role of *oca2* in melanin pigmentation in *Astyanax mexicanus*. *Dev. Biol.* **441**, 313–318. (doi:10.1016/j.ydbio.2018.03.014)
20. Edwards M, Bigham A, Tan J, Li S, Gozdzik A, Ross K, Jin L, Parra EJ. 2010 Association of the *OCA2* polymorphism His615Arg with melanin content in East Asian populations: further evidence of convergent evolution of skin pigmentation. *PLoS Genet.* **6**, e1000867. (doi:10.1371/journal.pgen.1000867)
21. Saenko SV, Lamichhaney S, Barrio AM, Rafati N, Andersson L, Milinkovitch MC. 2015 Amelanism in the corn snake is associated with the insertion of an LTR-retrotransposon in the OCA2 gene. *Sci. Rep.* **5**, 17118. (doi:10.1038/srep17118)
22. Protas ME, Hersey C, Kochanek D, Zhou Y, Wilkens H, Jeffery WR, Zon LI, Borowsky R, Tabin CJ. 2006 Genetic analysis of cavefish reveals molecular convergence in the evolution of albinism. *Nat. Genet.* **38**, 107–111. (doi:10.1038/ng1700)
23. Kratochwil CF, Urban S, Meyer A. 2019 Genome of the Malawi golden cichlid fish (*Melanochromis auratus*) reveals exon loss of *oca2* in an amelanistic morph. *Pigment Cell Melanoma Res.* **32**, 719–723. (doi:10.1111/pcmr.12799)
24. O'Gorman M *et al.* 2021 Pleiotropic function of the *oca2* gene underlies the evolution of sleep loss and albinism in cavefish. *Curr. Biol.* **31**, 3694-3701. (doi:10.1016/j.cub.2021.06.077)
25. Parichy DM. 2021 Evolution of pigment cells and patterns: recent insights from teleost fishes. *Curr. Opin. Genet. Dev.* **69**, 88–96. (doi:10.1016/j.gde.2021.02.006)
26. Kelsh RN, Barsh GS. 2011 A nervous origin for fish stripes. *PLoS Genet.* **7**, e1002081. (doi:10.1371/journal.pgen.1002081)
27. Parichy DM, Spiewak JE. 2015 Origins of adult pigmentation: diversity in pigment stem cell lineages and implications for pattern evolution. *Pigment Cell Melanoma Res.* **28**, 31–50. (doi:10.1111/pcmr.12332)
28. Singh AP, Nüsslein-Volhard C. 2015 Zebrafish stripes as a model for vertebrate colour pattern formation. *Curr. Biol.* **25**, R81–R92. (doi:10.1016/j.cub.2014.11.013)
29. Livraghi L *et al.* 2021 *Cortex cis*-regulatory switches establish scale colour identity and pattern diversity in *Heliconius*. *eLife* **10**, e68549. (doi:10.7554/eLife.68549)
30. Rasys AM, Park S, Ball RE, Alcala AJ, Lauderdale JD, Menke DB. 2019 CRISPR-Cas9 gene editing in lizards through microinjection of unfertilized oocytes. *Cell Rep.* **28**, 2288-2292. (doi:10.1016/j.celrep.2019.07.089)
31. Fang J, Chen T, Pan Q, Wang Q. 2018 Generation of albino medaka (*Oryzias latipes*) by CRISPR/Cas9. *J. Exp. Zool. B Mol. Dev. Evol.* **330**, 242–246. (doi:10.1002/jez.b.22808)
32. Li M *et al.* 2014 Efficient and heritable gene targeting in tilapia by CRISPR/Cas9. *Genetics* **197**, 591–599. (doi:10.1534/genetics.114.163667)
33. Wang C *et al.* 2021 Nile tilapia: a model for studying teleost color patterns. *J. Hered.* **112**, 469–484. (doi:10.1093/jhered/esab018)
34. Höch R, Schneider RF, Kickuth A, Meyer A, Woltering JM. 2021 Spiny and soft-rayed fin domains in acanthomorph fish are established through a BMP-gremlin-shh signaling network. *Proc. Natl Acad. Sci. USA* **118**, e2101783118. (doi:10.1073/pnas.2101783118)
35. Li CY, Steighner JR, Sweatt G, Thiele TR, Juntti SA. 2021 Manipulation of the *Tyrosinase* gene permits improved CRISPR/Cas editing and neural imaging in cichlid fish. *Sci. Rep.* **11**, 15138. (doi:10.1038/s41598-021-94577-8)
36. Wierson WA *et al.* 2020 Efficient targeted integration directed by short homology in zebrafish and mammalian cells. *eLife* **9**, e53968. (doi:10.7554/eLife.53968)
37. Kimura Y, Hisano Y, Kawahara A, Higashijima S. 2014 Efficient generation of knock-in transgenic zebrafish carrying reporter/driver genes by CRISPR/Cas9-mediated genome engineering. *Sci. Rep.* **4**, 6545. (doi:10.1038/srep06545)
38. Hisano Y, Sakuma T, Nakade S, Ohga R, Ota S, Okamoto H, Yamamoto T, Kawahara A. 2015 Precise in-frame integration of exogenous DNA mediated by CRISPR/Cas9 system in

zebrafish. *Sci. Rep.* **5**, 8841. (doi:10.1038/srep08841)

39. Li M, Liu X, Dai S, Xiao H, Wang D. 2019 High efficiency targeting of non-coding sequences using CRISPR/Cas9 system in tilapia. *G3 Genes Genomes Genet.* **9**, 287–295. (doi:10.1534/g3.118.200883)
40. Altschul SF, Gish W, Miller W, Myers EW, Lipman DJ. 1990 Basic local alignment search tool. *J. Mol. Biol.* **215**, 403–410. (doi:10.1016/S0022-2836(05)80360-2)
41. Varshney GK *et al.* 2015 High-throughput gene targeting and phenotyping in zebrafish using CRISPR/Cas9. *Genome Res.* **25**, 1030–1042. (doi:10.1101/gr.186379.114)
42. O'Quin KE, Smith D, Naseer Z, Schulte J, Engel SD, Loh YHE, Streelman JT, Boore JL, Carleton KL. 2011 Divergence in *cis*-regulatory sequences surrounding the opsin gene arrays of African cichlid fishes. *BMC Evol. Biol.* **11**, 120. (doi:10.1186/1471-2148-11-120)
43. Baldo L, Santos ME, Salzburger W. 2011 Comparative transcriptomics of Eastern African cichlid fishes shows signs of positive selection and a large contribution of untranslated regions to genetic diversity. *Genome Biol. Evol.* **3**, 443–455. (doi:10.1093/gbe/evr047)
44. Loh Y-HE, Yi SV, Streelman JT. 2011 Evolution of MicroRNAs and the diversification of species. *Genome Biol. Evol.* **3**, 55–65. (doi:10.1093/gbe/evq085)
45. Mayr C. 2017 Regulation by 3′-untranslated regions. *Annu. Rev. Genet.* **51**, 171–194. (doi:10.1146/annurev-genet-120116-024704)
46. Courtier-Orgogozo V, Arnoult L, Prigent SR, Wiltgen S, Martin A. 2020 Gephebase, a database of genotype–phenotype relationships for natural and domesticated variation in Eukaryotes. *Nucleic Acids Res.* **48**, D696–D703. (doi:10.1093/nar/gkz796)
47. Manga P, Boissy RE, Pifko-Hirst S, Zhou BK, Orlow SJ. 2001 Mislocalization of melanosomal proteins in melanocytes from mice with oculocutaneous albinism type 2. *Exp. Eye Res.* **72**, 695–710. (doi:10.1006/exer.2001.1006)
48. Costin GE, Valencia JC, Vieira WD, Lamoreux ML, Hearing VJ. 2003 Tyrosinase processing and intracellular trafficking is disrupted in mouse primary melanocytes carrying the *underwhite* (*uw*) mutation: a model for oculocutaneous albinism (OCA) type 4. *J. Cell Sci.* **116**, 3203–3212. (doi:10.1242/jcs.00598)
49. Patterson LB, Parichy DM. 2019 Zebrafish pigment pattern formation: insights into the development and evolution of adult form. *Annu. Rev. Genet.* **53**, 505–530. (doi:10.1146/annurev-genet-112618-043741)
50. Amiri MH, Shaheen HM. 2012 Chromatophores and color revelation in the blue variant of the Siamese fighting fish (*Betta splendens*). *Micron* **43**, 159–169. (doi:10.1016/j.micron.2011.07.002)
51. Owen JP, Kelsh RN, Yates CA. 2020 A quantitative modelling approach to zebrafish pigment pattern formation. *eLife* **9**, e52998. (doi:10.7554/eLife.52998)
52. Beeching SC, Glass BA, Rehorek SJ. 2013 Histology of melanic flank and opercular color pattern elements in the firemouth cichlid, *Thorichthys meeki*. *J. Morphol.* **274**, 743–749. (doi:10.1002/jmor.20131)
53. Mao Z, Bozzella M, Seluanov A, Gorbunova V. 2008 DNA repair by nonhomologous end joining and homologous recombination during cell cycle in human cells. *Cell Cycle* **7**, 2902–2906. (doi:10.4161/cc.7.18.6679)
54. Boel A, De Saffel H, Steyaert W, Callewaert B, De Paepe A, Coucke PJ, Willaert A. 2018 CRISPR/Cas9-mediated homology-directed repair by ssODNs in zebrafish induces complex mutational patterns resulting from genomic integration of repair-template fragments. *Dis. Model. Mech.* **11**, dmm035352. (doi:10.1242/dmm.035352)
55. Maruyama T, Dougan SK, Truttmann MC, Bilate AM, Ingram JR, Ploegh HL. 2015 Increasing the efficiency of precise genome editing with CRISPR-Cas9 by inhibition of nonhomologous end joining. *Nat. Biotechnol.* **33**, 538–542. (doi:10.1038/nbt.3190)
56. Malinsky M *et al.* 2015 Genomic islands of speciation separate cichlid ecomorphs in an East African crater lake. *Science* **350**, 1493–1498. (doi:10.1126/science.aac9927)
57. Munby H *et al.* 2021 Differential use of multiple genetic sex determination systems in divergent ecomorphs of an African crater lake cichlid. *BioRxiv* (doi:10.1101/2021.08.05.455235)
58. Joyce DA, Lunt DH, Genner MJ, Turner GF, Bills R, Seehausen O. 2011 Repeated colonization and hybridization in Lake Malawi cichlids. *Curr. Biol.* **21**, R108–R109. (doi:10.1016/j.cub.2010.11.029)
59. Kautt AF *et al.* 2020 Contrasting signatures of genomic divergence during sympatric speciation. *Nature* **588**, 106–111. (doi:10.1038/s41586-020-2845-0)
60. Clark B, Elkin J, Marconi A, Turner GF, Smith AM, Joyce D, Miska EA, Juntti SA, Santos ME. 2022 *Oca2* targeting using CRISPR/Cas9 in the Malawi cichlid *Astatotilapia calliptera*. Figshare. (https://doi.org/10.6084/m9.figshare.c.5937119)